# Low-Density Parity Check Codes and Iterative Decoding for Long-Haul Optical Communication Systems

Bane Vasic, *Senior Member, IEEE,* Ivan B. Djordjevic, and Raymond K. Kostuk, *Member, IEEE, Fellow, OSA*

***Abstract*—A forward-error correction )FEC) scheme based on low-density parity check (LDPC) codes and iterative decoding using belief propagation in code graphs is presented in this paper. We show that LDPC codes provide a significant system performance improvement with respect to the state-of-the-art FEC schemes employed in optical communications systems. We present a class of structured codes based on mutually orthogonal Latin rectangles. Such codes have high rates and can lend themselves to very low-complexity encoder/decoder implementations. The system performance is further improved by a code design that eliminates short cycles in a graph employed in iterative decoding.**

***Index Terms*—Balanced incomplete block designs (BIBDs), belief propagation algorithm, forward-error correction (FEC), long-haul transmission, low-density parity check(LDPC) codes, optical communications.**

## I. Introduction

THE GROWTH in demands for multimedia and broad-band services has placed high demands on optical communications systems and networks [1]–[4]. These demands are expected to continue to increase as multimedia resolution and precision imaging requirements develop. To meet these challenges terrestrial optical fiber systems are currently operating at 10-Gb/s channel data rates and experimental systems at 40 Gb/s have been demonstrated over distances of several thousand kilometers [2]. Some of the main component issues that must be solved for these systems include techniques for ultradense-wavelength multiplexing and demultiplexing over a large optical band, compensation techniques for polarization-mode dispersion (PMD), and residual chromatic dispersion, and reducing sensitivity to optical nonlinearities in the fiber medium. A number of significant advances have been made on these hardware issues; however, improvements to communication system performance can also be made by other methods. For instance sophisticated forward-error control coding techniques have proven to be very effective in extending the limits of wireless communications. These algorithmic approaches are often much less expensive to implement than new material or device development. In many respects, the coding algorithms that are being applied to fiber-optic communication channels are lagging far behind other types of communication modalities. Although data flow through optical communication systems has increased tremendously, it has become widely recognized that a full utilization of the available bandwidth cannot be achieved without powerful error-control schemes.

There has been a great deal of research activity in the area of error control coding during the last few years, ignited by the excellent bit-error rate (BER) performance of the turbo decoding algorithm demonstrated by Berrou and Glavieux [7]. Unfortunately, the turbo decoding is not suitable for optical communications because of its very high complexity of the Bahl, Cocke, Jelinek and Raviv (BCJR) algorithm [8], which is a main ingredient of the turbo decoder. Fortunately, during the last several years, turbo decoding has been generalized and mathematically formulated through the concept of codes on graphs. The prime examples of codes on graphs are low-density parity check (LDPC) codes. Extensive simulation results showed that, in many channels (such as additive white-noise Gaussian (AWGN) channel, binary symmetric channel, and erasure channel), LDPC codes perform nearly as well as earlier developed turbo codes. The theory of codes on graphs has not only improved the error performance, but has also opened new research avenues for investigating alternative suboptimal decoding schemes, such as belief propagation. The belief propagation algorithms and graphical models have been developed in the expert systems literature by Pearl [9] and, in the case of LDPC codes, are at least an order of magnitude simpler than the turbo decoding algorithm.

In this paper, we show that LDPC codes and iterative decoding based on belief propagation provide a significant system performance enhancement with respect to the state-of-the-art forward-error correction (FEC) schemes employed in optical communications systems.

An efficient algorithm that eliminates short cycles in a graph employed in iterative decoding, proposed here, allows further performance improvement. Namely, we exploit the idea that a judicious selection of disregarded blocks can also increase the girth of a design (or more precisely, the girth of a design bipartite graph). It is a desirable property of a bipartite graph to have a large girth, because the message-passing decoding algorithm on such graphs will perform better. The reason is that it takes more iterations until extrinsic information originating from different nodes in the bipartite graph becomes correlated.

## II. A Novel FEC Based on LDPC Codes

A significant effort has been made to apply FEC coding techniques to optical transmission systems starting with

Manuscript received April 15, 2002; revised June 24, 2002.

The authors are with the Department of Electrical and Computer Engineering, University of Arizona, Tucson, AZ 85721 USA. (e-mail: vasic@ece.arizona.edu; ivan@ece.arizona.edu; kostuk@ece.arizona.edu).

Digital Object Identifier 10.1109/JLT.2003.808769

Grover's proposal of applying FEC codes to dispersion-limited lightwave systems with laser impairments [10]. Recently, particularly in transoceanic submarine systems, error-correcting codes, such as the Bose–Chandhuri–Hocquenghem (BCH) code or the Reed–Solomon (RS) code have been selected for implementation [11]. Sab and Lemaire proposed using turbo codes for Alcatel long-haul submarine transmission system [12]. The transmission rate, error performance, and decoder hardware complexity can be further improved by using powerful error-control codes, in particular LDPC codes. To our knowledge, there is no published work on this subject.

We propose a scheme in which presently used Hamming and BCH codes are replaced by LDPC codes. In theory, the very long LDPC code approach is superior to both BCH and Hamming codes, but none of the existing literature on LDPC codes offers codes appropriate for the targeted application, which seeks multi-gigabit-per-second operation. Two the most important requirements for LDPC codes in optical communications are high code rate and simple encoder and decoder. The existing LDPC codes have large and "random" parity check matrices [16]. The implementation of such LDPC encoder/decoder is too complex and require too much memory to fit on a single chip.

We have demonstrated [13]–[15] that good codes can be constructed without using random sparse parity check matrices. The structure of our codes is of crucial importance for high-speed implementations, because these codes can lend themselves to extremely simple encoders, and because we can be assured of large minimum codeword distances. Since the spectral efficiency must stay high, we are interested in high-rate structured codes. The structure can also be used to provide flexible error protection, although this feature is not discussed in this paper. We showed that these codes can be efficiently decoded by belief propagation in associate bipartite graphs, because short cycles in a bipartite graph are eliminated. In this paper, system performance is further improved by using a special class of LDPC codes of even higher girth (shortest cycle length).

## III. Code Construction

The code construction presented in this paper is based on balanced incomplete block designs (BIBDs) [13], in particular, constructed from mutually orthogonal latin rectangles (MOLRs). The idea is to construct a combinatorial design, which is a structure that consists of a given number of points and subsets of these points, so-called blocks, and then to define a parity check matrix of a code as an incidence matrix between points and blocks in such a structure. Under certain conditions, such a parity check matrix defines an LDPC code. If a design is a BIBD, then all cycles of length four in a bipartite graph are eliminated, all parity checks are orthogonal, and a belief propagation algorithm can be used for decoding. We also give a class of codes that eliminates all cycles of length six, which further improves performance of belief propagation decoding.

### A. MOLR-Based Construction

In general, in combinatorics, a *design* is a pair $(V, B)$, where $V$ is a set of some elements called points, and $B$ is a collection of subsets of $V$ called blocks. The numbers of points and blocks are denoted by $v = |V|$ and $b = |B|$, respectively. If $t \leq v$ is an integer parameter, such that any subset of $t$ points from $V$ is contained in exactly $\lambda$ blocks, we deal with a $t$ design. A BIBD is a $t$-design for which each block contains the same number of points $k$, and every point is contained in the same number of blocks $r$. In this paper, we consider only BIBD with $t = 2$. Although such a BIBD still has five integer parameters $v$, $k$, $\lambda$, $b$ and $r$, only three of them are independent. Namely, the BIBD parameters satisfy the following two equations [15]: $vr = bk$ and $\lambda(v-1) = r(k-1)$. The notation $(v, k, \lambda)$-BIBD is used for a BIBD with $v$ points, block size $k$, index $\lambda$, and $t = 2$. A design is resolvable if there exists a nontrivial partition of its blocks set $B$ into parallel classes, each of which partitions the point set $V$. For example, the collection of blocks $B = \{\{1,2,3\},\{4,5,6\},\{7,8,9\},\{1,4,7\},\{2,5,8\},\{3,6,9\},\{1,5,9\},\{2,6,7\},\{3,4,8\},\{1,6,8\},\{2,4,9\},\{3,5,7\}\}$ is a 2-design with parameters $v = 9$, $b = 12$, and $\lambda = 1$. It is a resolvable design with four resolvability classes, each containing three blocks. The first resolvability class is $\{\{1,2,3\},\{4,5,6\},\{7,8,9\}\}$. As we will see later, the "lines" of the MOLR also form a resolvable BIBD. Given a design, a parity check matrix can be obtained as a point-block incidence matrix of the design. In other words, the nonzero positions within the columns of $H$ are specified by blocks of a design. For our example, the parity check matrix is

$$H = \begin{bmatrix} 1 & 0 & 0 & 1 & 0 & 0 & 1 & 0 & 0 & 1 & 0 & 0 \\ 1 & 0 & 0 & 0 & 1 & 0 & 0 & 1 & 0 & 0 & 1 & 0 \\ 1 & 0 & 0 & 0 & 0 & 1 & 0 & 0 & 1 & 0 & 0 & 1 \\ 0 & 1 & 0 & 1 & 0 & 0 & 0 & 0 & 1 & 0 & 1 & 0 \\ 0 & 1 & 0 & 0 & 1 & 0 & 1 & 0 & 0 & 0 & 0 & 1 \\ 0 & 1 & 0 & 0 & 0 & 1 & 0 & 1 & 0 & 1 & 0 & 0 \\ 0 & 0 & 1 & 1 & 0 & 0 & 0 & 1 & 0 & 0 & 0 & 1 \\ 0 & 0 & 1 & 0 & 1 & 0 & 0 & 0 & 1 & 1 & 0 & 0 \end{bmatrix}.$$

From the fact that $H$ does not have a full rank, and from the relations $vr = bk$ and $\lambda(v-1) = r(k-1)$, it follows that the code rate $R = (b - \operatorname{rank}(H))/b$ is lower bounded by

$$R \geq \frac{\lambda \frac{v(v-1)}{k(k-1)} - v}{\lambda \frac{v(v-1)}{k(k-1)}}. \tag{1}$$

The similar formula holds for general $t$ designs, $t > 1$, as well. In this case, the number of blocks is $b = \lambda \binom{v}{t} / \binom{k}{t}$. The required code lengths $b$ for a given code rate for a $(v, k, 1)$-BIBD are shown in Fig. 1. If the required code rate is higher than 0.9, what is typically required for optical communications, it is impossible to construct code shorter than 500.

An important subclass of BIBDs are so-called infinite families [24, p. 67], which, as the name indicates, contain an infinite number of designs. The examples of these BIBDs include projective geometries, affine geometries, unitals, and Denniston designs (see [24]). The known infinite families of BIBD are listed in Table I [24]. Notice that Kou, Lin, and Fossorier construction of LDPC codes [25] is based on projective geometry, a design from this class. Fig. 1 shows a lower bound on code length as a function of a code rate for LDPC codes obtained by using infinite families from Table I. As it can be seen from Fig. 2, these

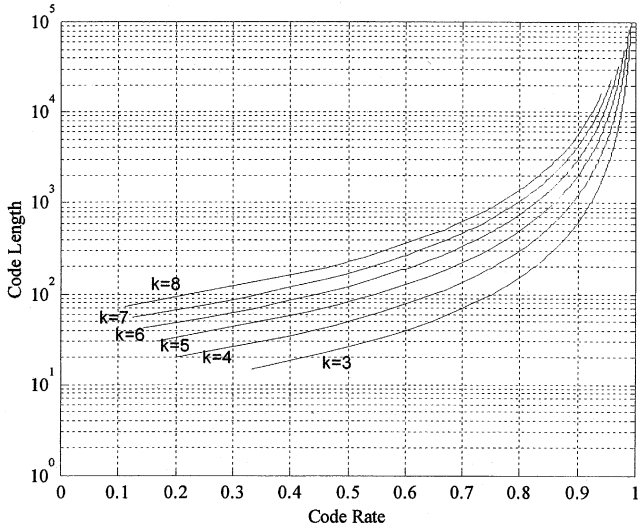


Fig. 1. Required codeword lengths of BIBD codes.

TABLE I
KNOWN INFINITE FAMILIES OF 2-$(v, k, 1)$ DESIGNS

| $k$ | $v$ | Parameter | Name |
|---|---|---|---|
| $q$ | $q^n$ | $n\geq 2$, $q$- a prime power | Affine geometries |
| $q+1$ | $(q^n-1)/(q-1)$ | $n\geq 2$, $q$- a prime power | Projective geometries |
| $q+1$ | $q^3+1$ | $q$- a prime power | Unitals |
| $2^m$ | $2^m(2^s+1)-2^s$ | $2\leq m<s$ | Denniston designs |

families offer quite a limited set of parameters (code lengths and column weights) and, therefore, a small class of codes in the high-rate, low-length region. This motivates the introduction of 2-$(v, k, 1)$ designs that have a flexible number of blocks $b$ and arbitrary block size $k$. The MOLR-based construction has exactly this property.

Now, we address the problem of construction of resolvable BIBDs using MOLR. This construction gives an extremely wide range of block sizes and code rates. It can be viewed as an extension on the integer lattice construction explained in [13]. A $m \times k$ integer array $[L_k(x,y)]_{1\leq x\leq k, 1\leq y\leq m}$ with elements $L_k(x,y)$ in $\{0,1,\ldots,m\}$ is referred to as *Latin rectangle* if each of the elements occurs once in each row and once in each column. For two rectangles $L_k^1 = \lfloor L_k^1(x,y)\rfloor_{1\leq x\leq k, 1\leq y\leq m}$ and $L_k^2 = \lfloor L_k^2(x,y)\rfloor_{1\leq x\leq k, 1\leq y\leq m}$, the *join* $\left(L_k^1, L_k^2\right)$ of $L_k^1$ and $L_k^2$ is the $mxk$ array whose $(x,y)$th entry is the pair $\left(L_k^1(x,y), L_k^2(x,y)\right)$. Two Latin rectangles $L_k^1$ and $L_k^2$ are *orthogonal* if all entries in the join are distinct (i.e., if $L_k^1(x,y) = L_k^2(x,y)$ and $L_k^1(X,Y) = L_k^2(X,Y)$, then $x = X$ and $y = Y$). Latin rectangles $L_k^1, L_k^2, \ldots, L_k^n$ are *mutually orthogonal* if they are orthogonal in pairs. The importance of such a property will be evident shortly. For the sake of simplicity, let us start with MOLRs of equal sizes (i.e., mutually orthogonal Latin rectangles). This construction is based on elementary combinatorics (see, e.g., [21]). Let the dimensions of squares be $k = m = p^l$, $p$ is a prime, $l \geq 1$, and let $\alpha_0 = 0, \alpha_1, \alpha_2, \ldots, \alpha_{k-1}$ be the elements of $GF(k)$. Consider the nonzero element $\alpha$ and define a $k \times k$ array $L_k^\alpha$ with elements $L_k^\alpha(x,y) = \alpha \cdot \alpha_x + \alpha_y$, $0 \leq x, y \leq k-1$. It can

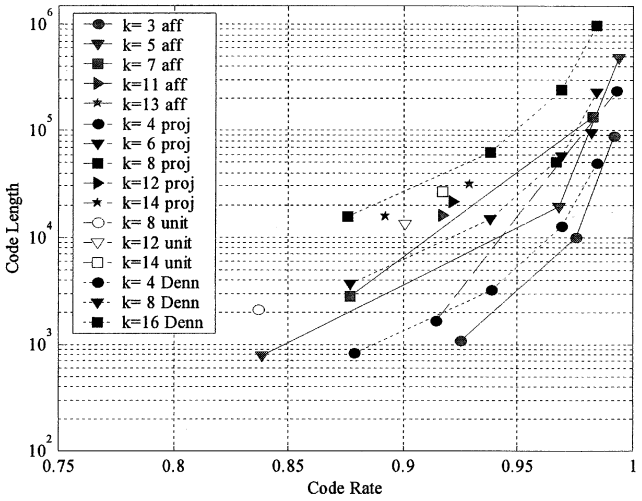


Fig. 2. Rate-length curves for known infinite $2-(v,k,1)$ families form Table I.

be shown that the arrays $L_k^\alpha$, $0 \leq x, y \leq k-1$ are mutually orthogonal Latin squares (MOLS) of order $k$ [24]. For example

$$L_4^1 = \begin{bmatrix} 0 & 1 & 2 & 3 \\ 1 & 0 & 3 & 2 \\ 2 & 3 & 0 & 1 \\ 3 & 2 & 1 & 0 \end{bmatrix}$$

$$L_4^2 = \begin{bmatrix} 0 & 1 & 2 & 3 \\ 2 & 3 & 0 & 1 \\ 3 & 2 & 1 & 0 \\ 1 & 0 & 3 & 2 \end{bmatrix}$$

$$L_4^3 = \begin{bmatrix} 0 & 1 & 2 & 3 \\ 3 & 2 & 1 & 0 \\ 1 & 0 & 3 & 2 \\ 2 & 3 & 0 & 1 \end{bmatrix}$$

are three MOLS of order four (indexes are used here to represent the elements of the $GF(4)$). Consider now a $k \times k$ integer lattice $L = Z_k \times Z_k$ with elements labeled by the points from the set $V$. In other words, let $l : L \to V$ be a one-to-one mapping of the square $L$ to the integer set $V$ of a design. An example of such mapping is a simple linear mapping $l(x,y) = m{\cdot}x+y+1$. The numbers $l(x,y)$ are referred to as *cell labels*. Each $L_k^\alpha$ defines a set of $k$ parallel lines $B_k^\alpha = \{l(x,y) : L_\alpha(x,y) = s\}$, $0 \leq s \leq k-1$. These sets are analogous to the sets of lines with slopes $1 \leq s \leq k-1$ in the lattice design introduced in [13]. The slopes $s = 0$ and $s = \infty$ can be also included to create a full resolvable BIBD with $v = k^2$, $b = k(k+1)$, and $r = k+1$. The corresponding design with the resolvability classes shown in different columns is given in Table II. Our experimental findings show, however, that excluding the infinite slope leads to better performance. Each line of a design specifies positions of nonzero elements in a column of parity check matrix $H$.

For example, the parity check matrix corresponding to the last four columns (slopes: $s = 0, \alpha_1, \alpha_2, \alpha_3$) in Table II is shown in the equation at the bottom of the next page.

Notice that each column in the Table II corresponds to a $kxk$ submatrix in $H$.

Consider now a Latin rectangle with horizontal and vertical dimensions equal to $k$ and $m$, respectively. To keep the ex-

TABLE II
LINES OF THE MOLR CONSTRUCTED FROM $GF(4)$

| s=∞ | s=0 | $\alpha_1$ | $\alpha_2$ | $\alpha_3$ |
|---|---|---|---|---|
| 1 2 3 4 | 1 5 9 13 | 1 6 11 16 | 1 8 10 15 | 1 7 12 14 |
| 5 6 7 8 | 2 6 10 14 | 2 5 12 15 | 4 5 11 14 | 3 5 10 16 |
| 9 10 11 12 | 3 7 11 15 | 3 8 9 14 | 2 7 9 16 | 4 6 9 15 |
| 13 14 15 16 | 4 8 12 16 | 4 7 10 13 | 3 6 12 13 | 2 8 11 13 |

position simple, we illustrate the construction for prime $m$. It can be readily extended to the case when $m$ is a prime power using the same approach as in the square case. For each $\alpha \in \{0, 1, \ldots, m-1\}$, we define the rectangle $L^{\alpha}_{k,m}$ with elements $L_{\alpha}(x, y) = \alpha \cdot x + y$. For example, the MOLR with $k = 3$ and $m = 7$ consists of the following seven rectangles:

$$L^0_{3,7} = \begin{bmatrix} 0 & 0 & 0 \\ 1 & 1 & 1 \\ 2 & 2 & 2 \\ 3 & 3 & 3 \\ 4 & 4 & 4 \\ 5 & 5 & 5 \\ 6 & 6 & 6 \end{bmatrix}$$

$$L^1_{3,7} = \begin{bmatrix} 0 & 1 & 2 \\ 1 & 2 & 3 \\ 2 & 3 & 4 \\ 3 & 4 & 5 \\ 4 & 5 & 6 \\ 5 & 6 & 0 \\ 6 & 0 & 1 \end{bmatrix}$$

$$L^2_{3,7} = \begin{bmatrix} 0 & 2 & 4 \\ 1 & 3 & 5 \\ 2 & 4 & 6 \\ 3 & 5 & 0 \\ 4 & 6 & 1 \\ 5 & 0 & 2 \\ 6 & 1 & 3 \end{bmatrix}$$

$$L^3_{3,7} = \begin{bmatrix} 0 & 3 & 6 \\ 1 & 4 & 0 \\ 2 & 5 & 1 \\ 3 & 6 & 2 \\ 4 & 0 & 3 \\ 5 & 1 & 4 \\ 6 & 2 & 5 \end{bmatrix}$$

$$L^4_{3,7} = \begin{bmatrix} 0 & 4 & 1 \\ 1 & 5 & 2 \\ 2 & 6 & 3 \\ 3 & 0 & 4 \\ 4 & 1 & 5 \\ 5 & 2 & 6 \\ 6 & 3 & 0 \end{bmatrix}$$

$$L^5_{3,7} = \begin{bmatrix} 0 & 5 & 3 \\ 1 & 6 & 4 \\ 2 & 0 & 5 \\ 3 & 1 & 6 \\ 4 & 2 & 0 \\ 5 & 3 & 1 \\ 6 & 4 & 2 \end{bmatrix}$$

$$L^6_{3,7} = \begin{bmatrix} 0 & 6 & 5 \\ 1 & 0 & 6 \\ 2 & 1 & 0 \\ 3 & 2 & 1 \\ 4 & 3 & 2 \\ 5 & 4 & 3 \\ 6 & 5 & 4 \end{bmatrix}.$$

Notice that we allow the occurrence of same elements in rows of the first rectangle, which means that, strictly speaking, the first rectangle is not Latin. In general, there are $m$ parallel classes of lines, each corresponding to different $\alpha$. As in the case of Latin squares, each rectangle $L^{\alpha}_{k,m}$ defines a set of parallel lines $B^{\alpha}_{k,m} = \{l(x, y) : L_{\alpha}(x, y) = s, 0 \leq s \leq m-1$. Notice that some pairs of points are not contained in any line, which means that the design is imbalanced and that the design index $\lambda$ can be either zero or one. Again, the lines determine

$$H = \begin{bmatrix} 1 & 0 & 0 & 0 & 1 & 0 & 0 & 0 & 1 & 0 & 0 & 0 & 1 & 0 & 0 & 0 \\ 0 & 1 & 0 & 0 & 0 & 1 & 0 & 0 & 0 & 0 & 1 & 0 & 0 & 0 & 0 & 1 \\ 0 & 0 & 1 & 0 & 0 & 0 & 1 & 0 & 0 & 0 & 0 & 1 & 0 & 1 & 0 & 0 \\ 0 & 0 & 0 & 1 & 0 & 0 & 0 & 1 & 0 & 1 & 0 & 0 & 0 & 0 & 1 & 0 \\ 1 & 0 & 0 & 0 & 0 & 1 & 0 & 0 & 0 & 1 & 0 & 0 & 0 & 1 & 0 & 0 \\ 0 & 1 & 0 & 0 & 1 & 0 & 0 & 0 & 0 & 0 & 0 & 1 & 0 & 0 & 1 & 0 \\ 0 & 0 & 1 & 0 & 0 & 0 & 0 & 1 & 0 & 0 & 1 & 0 & 1 & 0 & 0 & 0 \\ 0 & 0 & 0 & 1 & 0 & 0 & 1 & 0 & 1 & 0 & 0 & 0 & 0 & 0 & 0 & 1 \\ 1 & 0 & 0 & 0 & 0 & 0 & 1 & 0 & 0 & 0 & 1 & 0 & 0 & 0 & 1 & 0 \\ 0 & 1 & 0 & 0 & 0 & 0 & 0 & 1 & 1 & 0 & 0 & 0 & 0 & 1 & 0 & 0 \\ 0 & 0 & 1 & 0 & 1 & 0 & 0 & 0 & 0 & 1 & 0 & 0 & 0 & 0 & 0 & 1 \\ 0 & 0 & 0 & 1 & 0 & 1 & 0 & 0 & 0 & 0 & 0 & 1 & 1 & 0 & 0 & 0 \\ 1 & 0 & 0 & 0 & 0 & 0 & 0 & 1 & 0 & 0 & 0 & 1 & 0 & 0 & 0 & 1 \\ 0 & 1 & 0 & 0 & 0 & 0 & 1 & 0 & 0 & 1 & 0 & 0 & 1 & 0 & 0 & 0 \\ 0 & 0 & 1 & 0 & 0 & 1 & 0 & 0 & 1 & 0 & 0 & 0 & 0 & 0 & 1 & 0 \\ 0 & 0 & 0 & 1 & 1 & 0 & 0 & 0 & 0 & 0 & 1 & 0 & 0 & 1 & 0 & 0 \end{bmatrix}$$

TABLE III
AN EXAMPLE OF AN MOLR 2-DESIGN

| s=0 | s=1 | s=2 | s=3 | s=4 | s=5 | s=6 |
|---|---|---|---|---|---|---|
| 1 8 15 | 1 14 20 | 1 13 18 | 1 12 16 | 1 11 21 | 1 10 19 | 1 9 17 |
| 2 9 16 | 2 8 21 | 2 14 19 | 2 13 17 | 2 12 15 | 2 11 20 | 2 10 18 |
| 3 10 17 | 3 9 15 | 3 8 20 | 3 14 18 | 3 13 16 | 3 12 21 | 3 11 19 |
| 4 11 18 | 4 10 16 | 4 9 21 | 4 8 19 | 4 14 17 | 4 13 15 | 4 12 20 |
| 5 12 19 | 5 11 17 | 5 10 15 | 5 9 20 | 5 8 18 | 5 14 16 | 5 13 21 |
| 6 13 20 | 6 12 18 | 6 11 16 | 6 10 21 | 6 9 19 | 6 8 17 | 6 14 15 |
| 7 14 21 | 7 13 19 | 7 12 17 | 7 11 15 | 7 10 20 | 7 9 18 | 7 8 16 |

the positions of ones in columns of $H$. Table III gives the lines (positions of ones in columns of $H$) for our example.

Generally, the parity check matrix of MOLR codes can be written in the form

$$H = \begin{bmatrix} H_{1,1} & H_{1,2} & \dots & H_{1,m} \\ H_{2,1} & H_{2,2} & \dots & H_{2,m} \\ \vdots & \vdots & & \vdots \\ H_{k,1} & H_{k,2} & \dots & H_{k,m} \end{bmatrix} \tag{2}$$

where each submatrix is a permutation matrix.

Notice that $H$ has exactly the same form as proposed by Gallager [26]. The MacKay's regular LDPC codes [16], [22], [31] are in fact the special case of our MOLR-based codes. Namely, by random permutations of the columns of the parity check matrix of a MOLR code (and including lines with infinite slope), we can obtain MacKay, as well as many other random codes. However, since all these codes are structurally identical, they will perform exactly the same in the AWGN channel.

The decoding complexity (in the algorithmic sense) of MacKay's LDPC codes is comparable to the MOLR-based LDPC class, since the same sum-product (message-passing or belief propagation) algorithm is used in decoding (as explained in Section IV). However, the regular structure of MOLR codes allows for reduced-complexity architectures. A decoding architecture for finite-geometry LDPC codes has been recently presented by Yeo *et al.* [27]. Another (so-called vector LDPC) architecture has been recently implemented and is now commercially available in Flarion LDPC chip [28]. The third example of a structured-code architecture that is also commercially available is Agere LDPC chip [29]. The encoding complexity of structured LDPC codes is also lower compared with random codes. One such encoder architecture has been proposed by Vasic [13]. Parity check matrices of designs with equal number of points and blocks (so-called symmetric designs) can be written in a cyclic form and encoded by a linear shift register circuitry [25].

Although it is known from work of Kschischang–Frey that short cycles hurt the convergence of LDPC codes, recently Richardson *et al.*[30] provided analytical evidence that the elimination of short cycles actually lowers the error floor. Since the error floor in optical communication systems is much lower compared with wireless systems, it is desirable that an LDPC code does not have short cycles, or that there is a systematic way of eliminating short cycles. Section III-B offers such a construction based on MOLR.

### B. 2-$(v, k, 1)$ Girth-Eight Designs

Denote by $B(s)$ a resolvability class corresponding to MOLR of slope $s$, and by $B'$ a set of blocks of a sub-design composed of resolvability classes corresponding to the slopes from the set $S$, i.e., $B' = \cup_{s \in S} B(s)$. We are interested in the following problem: find a maximum cardinality slope set $S$ such that $B'$ is a girth-eight design. The algorithm for finding a girth-eight subdesign $(V, B')$ is as follows:

$s = 0,\ S = \{s\},\ B' = B(s),\ S' = \{1, \dots, m-1\}.$
`while` $S' \neq \emptyset$
$s = s + 1$
`if` $g(V, B' \cup B(s)) = 8$
 $S = S \cup \{s\}$
 $S' = S' \backslash \{s\}$
 $B' = B' \cup B(s)$
`else`
 $S' = S' \backslash \{s\}$
`end`
`end.`

The function $g : (V, B) \to Z_+$ gives the girth of a graph and can be computed in time linear in $|V|$ (see [20]).

## IV. BELIEF PROPAGATION ALGORITHM

For any codeword $x = (x_v)_{1 \le v \le n}$ in a linear block code given by the parity check matrix $H$, the following set of equations is satisfied:

$$\sum_v h_{c,v} \cdot x_c = 0, \quad 1 \le c \le n - k. \tag{3}$$

The above equations are called parity check equations. Iterative decoding can be visualized as message passing on a bipartite graph representation of the parity check matrix [17]. There are two types of vertices in the graph: check vertices (check nodes) indexed by $c$ and variable vertices (bit nodes) indexed by $v$. Edge-connecting vertices $c$ and $v$ exist if $h_{c,v} = 1$, i.e., if variable $v$ participates in the parity check equation $c$. For example, the bipartite graph corresponding to

$$H = \begin{bmatrix} 1 & 0 & 0 & 0 & 1 & 0 & 1 \\ 1 & 1 & 0 & 0 & 0 & 1 & 0 \\ 0 & 1 & 1 & 0 & 0 & 0 & 1 \\ 1 & 0 & 1 & 1 & 0 & 0 & 0 \\ 0 & 1 & 0 & 1 & 1 & 0 & 0 \\ 0 & 0 & 1 & 0 & 1 & 1 & 0 \\ 0 & 0 & 0 & 1 & 0 & 1 & 1 \end{bmatrix}$$

is shown in Fig. 3. In Fig. 3, each row is represented by a square (a parity check equation), referred to as a check node, while the

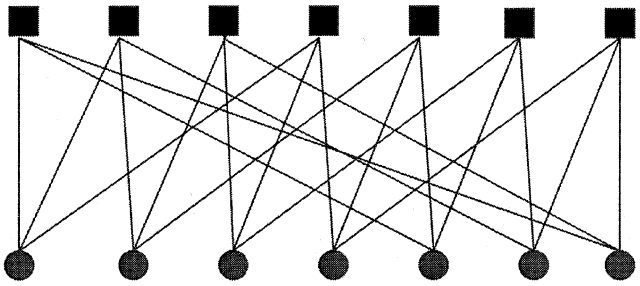

Fig. 3. An example of a bipartite graph.

bits in a check are represented by the circles referred to as bit nodes.

Decoding can be done as follows. First, *a priori* information of the bit at position $v(a_v)$, $\mu_v^{(0)} = \log(P(a_v = 1)/P(a_v = 0))$ is obtained from the channel detector, and values associated with every edge $(c, v)$ in the bipartite graph $\lambda_{c,v}^{(j)}$ are initialized to zero. In $j$th iteration, we update the values $\lambda_{c,v}^{(j)}$ according to:

$$\lambda_{c,v}^{(j)} = 2(-1)^{\sum_w h_{c,w}} \tanh^{-1} \times \left( \prod_{w \neq v} \tanh \left( \frac{\mu_w^{(j-1)} - \lambda_{c,w}^{(j-1)}}{2} \right) \right). \quad (4)$$

The last step in iteration $j$ is to compute the updated likelihood ratios $\mu_v^{(j)}$ according to

$$\mu_v^{(j)} = \mu_v^{(0)} + \sum_c \lambda_{c,v}^{(j)}. \quad (5)$$

Decoding halts when a valid codeword or a maximum number of iteration has been reached. Steps (4) and (5) can be viewed as propagation of likelihoods (beliefs) in a code bipartite graph [13], [17].

It is desirable to have each bit "checked" in as many equations as possible, but because of the iterative nature of the decoding algorithm, the bipartite graph must not contain short cycles. In other words, the graph *girth* (the length of the shortest cycle) must be large. These two requirements are contradictory, and the tradeoff is especially difficult when we want to construct a code that is both short and has a high rate. As explained in Section II, in a BIBD, no two blocks contain the same pair of points, and consequently, the corresponding bipartite graph has girth six, which supports the belief propagation algorithm [17]. Algorithm proposed in Section III-B increases the girth of a design bipartite graph. As we show in Section V, the belief propagation decoding algorithm on such graphs performs better. Namely, it takes more iterations until extrinsic information originating from different nodes in the bipartite graph becomes correlated.

## V. LDPC Code Performance

The main impairments in long-haul optical transmission come from amplified spontaneous emission (ASE) noise, pulse distortion due to fiber nonlinearities, chromatic dispersion or polarization dispersion, crosstalk effects, intersymbol interference (ISI), etc. The models presented so far [11], [12], [18] in considering the FEC are based on the AWGN assumption. In contrast, our simulator allows for taking into account in a natural way all major impairments in a long-haul optical transmission, such as ASE noise, pulse distortion due to fiber nonlinearities, chromatic dispersion or polarization dispersion, crosstalk effects, ISI, etc. In addition, it can be used to analyze a variety of FEC schemes, especially those based on iterative decoding.

In this section, we study the performance of LDPC codes in the presence of residual dispersion, fiber nonlinearities, ISI and receiver noise resulting from signal–noise and noise–noise interaction on a p-i-n photodiode. The influence of the transfer functions of optical and electrical filters is taken into account as well. A wavelength-division-multiplexing (WDM) system with a 10-Gb/s bit rate per channel and a channel spacing of 50 GHz is considered. It is assumed that the observed channel is located at 1552.524 nm (193.1 THz) and that there exists a nonnegligible interaction with six neighboring channels. The extinction ratio is set to 13 dB. The transmitter and receiver imperfection is described through a back-to-back $Q$ factor, which is set to 23 dB.

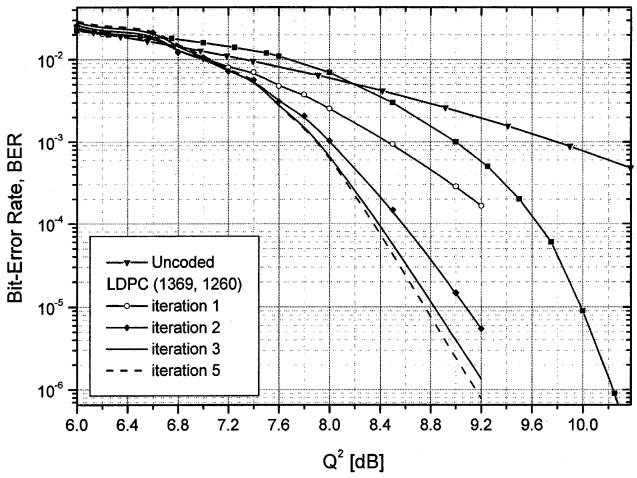


Fig. 4. BER performance of MOLR-based LDPC (1369, 1260) code for the AWGN channel.

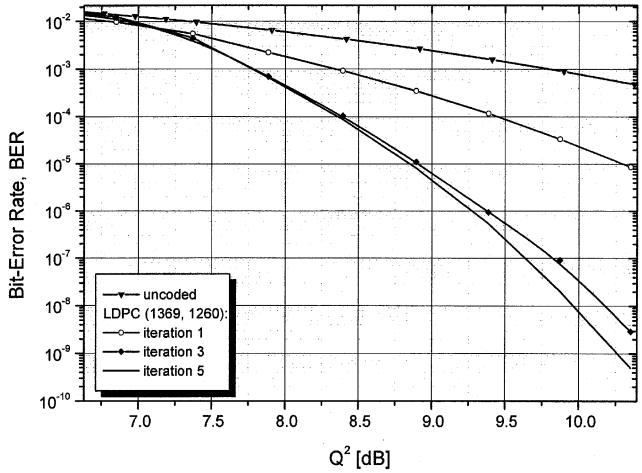


Fig. 5. BER performance of MOLR-based LDPC (1369, 1260) code, including the transmission medium and a realistic receiver model.

The results of a Monte Carlo simulation for the MOLR-based LDPC (1369,1260) code with a code rate of $R = 0.92$ (redundancy of 8.7%) and the AWGN channel are shown in Fig. 4. For $10^{-6}$, the LDPC (1369,1260) scheme outperforms the RS (255 239) code by 1.1 dB.

Fig. 5 shows the BER results of a Monte Carlo simulation for a typical receiver comprised of an erbium-doped fiber amplifier (EDFA) as a preamplifier, an optical filter (modeled as a super-Gaussian filter of the eighth order and bandwidth $2R_b$, $R_b$ bit rate over code rate), a p-i-n photodiode, an electrical filter (modeled as a Gaussian filter of bandwidth $0.65R_b$), a sampler and a decision circuit. The transmission

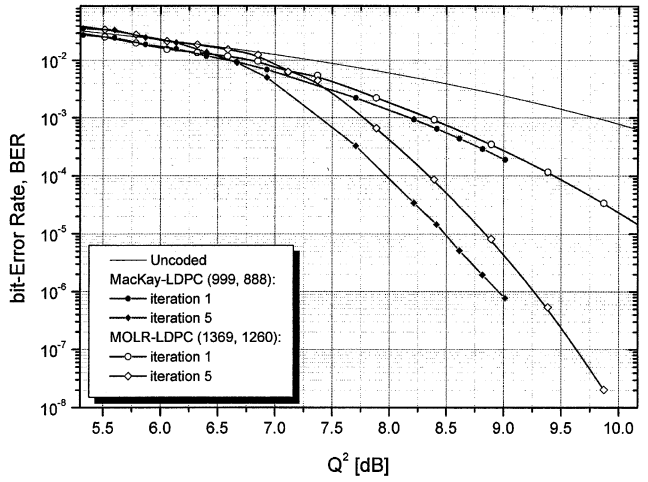


Fig. 6. MOLR-based LDPC (1369, 1260) code versus MacKay's LDPC (999, 888) upon transmission.

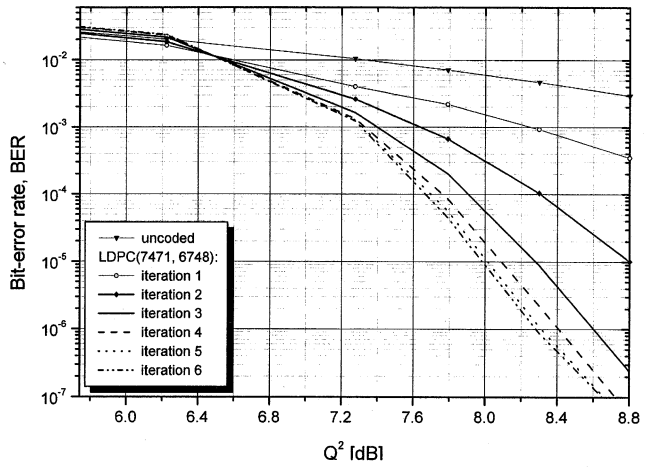


Fig. 7. BER performance of MOLR-based LDPC (7471, 6748) code of girth eight.

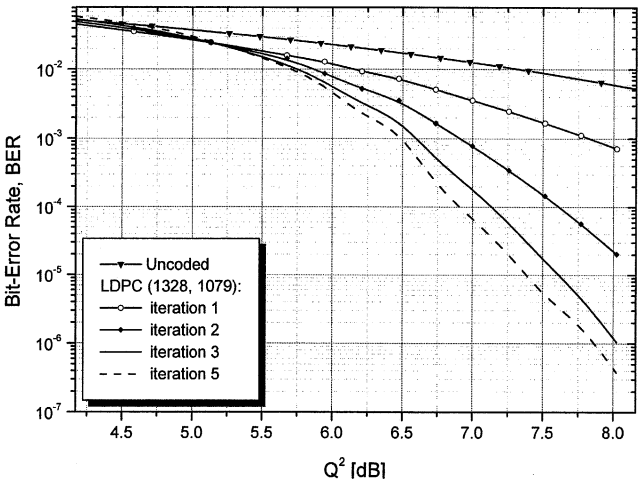


Fig. 8. BER performance of MOLR-based LDPC (1328, 1079) code of girth eight.

with the dispersion map composed of standard single-mode fiber (SMF) and dispersion-compensating fiber (DCF) sections giving the residual dispersion of 272 ps/nm is considered. The average power per channel of 0 dBm and a nonreturn-to-zero (NRZ) format are assumed. The SMF attenuation coefficient, dispersion, dispersion slope, nonlinear refractive index, and effective cross-sectional area are set to 0.21 dB/km, 17 ps $nm^{-1}$ $km^{-1}$, 0.065 ps $nm^{-2}$ $km^{-1}$, $2.6 \cdot 10^{-20}$ $m^2/W$, and 80 $\mu m^2$, respectively. Corresponding DCF parameters are 0.5 dB/km, $-100$ ps $nm^{-1}$ $km^{-1}$, $-0.33$ ps $nm^{-2}$ $km^{-1}$, $2.6 \cdot 10^{-20}$ $m^2/W$, and 30 $\mu m^2$.

The comparison with MacKay's regular LPDC codes [16], [22], [31], which are frequently used as a reference in coding literature, is given in Fig. 6. For $10^{-6}$, the MacKay's LDPC code outperforms MOLR for $\sim$0.3 dB. Notice that that the performance difference between the MOLR-based LDPC code (1369, 1260) and MacKay's regular LDPC (999, 888) code diminishes at lower BERs. We expect the MOLR-based LDPC codes to perform better for BERs lower than $10^{-9}$. The discrepancy for higher BERs also come from the fact that the MacKay's LDPC (999, 888) code has higher redundancy ($\sim$12.5%) than MOLR-based LDPC (1369, 1260) code ($\sim$8.7%). MOLR-based LDPC codes of girth eight significantly outperform (see Figs. 7 and 8) MacKay's regular LDPC codes. Further improvement of MOLR-based LDPC codes is possible by random permutations of columns in the parity check matrix. Unfortunately, random column permutation destroys the structure of a parity check matrix (2), which results in increased encoder/decoder complexity [26].

The results for LDPC codes of girth eight are shown in Figs. 7 and 8, upon transmission. For $10^{-6}$, the LDPC (7471, 6748) scheme (Fig. 7) outperforms the RS (255 239) code by 2 dB, and the LDPC (1328, 1079) (Fig. 8) by 2.5 dB. (More details on RS/turbo code performance in optical communications can be found in [11].) Much more complex block turbo code based on a product of two BCH (128,113,6) codes, with 3-b quantized samples and with 28% redundance, gives performace comparable to our LDPC (7471, 6748). Notice that our code has much smaller redundance ($\sim$10%). Notice also that the complexity of the RS/turbo decoder is much higher than that of a LDPC decoder of equal or comparable length. Another important observation is that coding gain at lower BER (not shown in the figure) will be larger because of a steeper waterfall curve of LDPC codes [15].

## VI. Conclusion

We have presented an FEC scheme based on LDPC codes. We demonstrate a significant coding gain of LDPC with respect to the state-of-the-art FEC schemes employed in optical communications systems. These codes have many unique features that may allow for very high-speed implementations. For example Hagenauer *et al.* [19] realized that the sum-product algorithm is well suited for analog very large scale integratin (VLSI) implementation. Not only does the code graph specify a natural layout, but also the sum-product operations are well matched to the natural nonlinear physical behavior of transistors. This kind of fast analog iterative decoder is a very attractive option for optical communications.

To improve overall system performances these new LDPC schemes can also be considered in conjunction with traditional

algebraic decoding schemes, such as BCH and RS codes, which may be required to further lower the BER. This approach is valuable not only because most of today's systems use algebraic codes, but also because the error floor of the LDPC in the presence of burst of errors due to nonlinearities and signal-dependent noise has not yet been assessed. These and the issues of high-rate code constructions are left for the future research.

## REFERENCES


[1] G. Vareille, B. Julien, F. Pitel, and J. F. Marcerou, "3.65 Tb/s (365 × 11.6 Gb/s) transmission experiment over 6850 km using 22.2 GHz channel spacing in NRZ format," in *Proc. 27th European Conf. Optical Communication*, vol. 6, 2001, pp. 14–15.

[2] J.-X. Cai, M. Nissov, A. N. Pilipetskii, M. A. Mills, L. Xu, D. Foursa, P. C. Corbet, D. Sutton, and N. S. Bergano, "1.28 Tb/s (32 × 40 Gb/s) transmission over 4,500 km," in *Proc. 27th European Conf. Optical Communication*, vol. 6, 2001, pp. 4–5.

[3] M. Arend, D. Duff, E. Golovchenko, A. Pilipetskii, K. Razavi, D. Sliwinski, M. Vaa, W. W. Patterson, and B. Bakhshi, "Advantages of orthogonal polarization launch in a 6500 km straight-line DWDM transmission experiment," presented at the Optical Fiber Communication Conf. 2002, Anaheim, CA, USA, Mar. 19–21, 2002.

[4] D. F. Grosz, A. Küng, D. N. Maywar, L. Altman, M. Movassaghi, H. C. Lin, D. A. Fishman, and T. H. Wood, "Demonstration of all-Raman ultra-wide-band transmission of 1.28 Tb/s (128 × 10 Gb/s) over 4000 km of NZ-DSF with large BER margins," in *Proc. 27th European Conf. Optical Communication*, vol. 6, 2001, pp. 72–73.

[5] A. Hodzic, B. Konrad, and K. Petermann, "Prechirp in NRZ-based 40-Gb/s single-channel and WDM transmission systems," *IEEE Photon. Technol. Lett.*, vol. 14, pp. 152–154, Feb. 2002.

[6] K. Kumano, K. Mukasa, M. Sakano, H. Moridaira, T. Yagi, and K. Kokura, "Novel NZ-DSF with ultra-low dispersion slope lower than 0.020 ps/nm$^2$/km," in *Proc. 27th European Conf. Optical Communication*, vol. 6, 2001, pp. 48–49.

[7] C. Berrou and A. Glavieux, "Near optimum error-correcting coding and decoding: Turbo codes," *IEEE Trans. Commun.*, vol. 44, pp. 1261–1271, Oct. 1996.

[8] L. R. Bahl, J. Cocke, F. Jelinek, and J. Raviv, "Optimal decoding of linear codes for minimizing symbol error rate," *IEEE Trans. Inform. Theory*, vol. IT-20, pp. 284–287, Mar. 1974.

[9] J. Pearl, *Probabilistic Reasoning in Intelligent Systems: Networks of Plausible Inference*. San Mateo, CA: Morgan Kaufmann, 1988.

[10] W. D. Grover, "Forward error correction in dispersion-limited lightwave systems," *J. Lightwave Technol.*, vol. 6, pp. 643–654, May 1988.

[11] O. A. Sab, "FEC techniques in submarine transmission systems," in *Proc. Optical Fiber Communication Conf.*, vol. 2, 2001, pp. TuF1-1–TuF1-3.

[12] O. A. Sab and V. Lemaire, "Block turbo code performances for long-haul DWDM optical transmission systems," in *Proc. Optical Fiber Communication Conf. 2000*, vol. 3, 2000, pp. 280–282.

[13] B. Vasic, "Combinatorial construction of low-density parity check codes," presented at the Int. Symp. Information Theory, Lausanne, Switzerland, June–July 30–5, 2002.

[14] B. Vasic, E. Kurtas, and A. Kuznetsov, "Lattice low-density parity check codes and their application in partial response channels," presented at the Int. Symp. Information Theory, Lausanne, Switzerland, June–July 30–5, 2002.

[15] B. Vasic, "Combinatorial constructions of structured low-density parity check codes for iterative decoding," *IEEE Trans. Inform. Theory*, to be published.

[16] D. J. C. MacKay, "Good error-correcting codes based on very sparse matrices," *IEEE Trans. Inform. Theory*, vol. 45, pp. 399–431, Mar. 1999.

[17] F. R. Kschischang and B. J. Frey, "Iterative decoding of compound codes by probability propagation in graphical models," *IEEE J. Select. Areas Commun.*, vol. 16, pp. 219–230, Feb. 1998.

[18] H. Kidorf, N. Ramanujam, I. Hayee, J.-X. Cai, B. Pedersen, A. Puc, and C. Rivers, "Performance improvement using forward error correction codes," in *Proc. Optical Fiber Communication Conf. 2000*, vol. 3, 2000, pp. ThS3-1–ThS3-3.

[19] J. Hagenauer, M. Moerz, and E. Offer, "Analog turbo-networks in VLSI: The next step in turbo decoding and equalization," presented at the 2nd Int. Symp. Turbo Codes, Brest, France, Sept. 4–7, 2000.

[20] T. H. Cormen, C. E. Leiserdon, and R. L. Rivest, *Introduction to Algorithms*. Cambridge, MA: McGraw-Hill, 1989.

[21] J. H. van Lint and R. M. Wilson, *A Course in Combinatorics*. Cambridge, U.K.: Cambridge Univ. Press, 1992.

[22] D. J. C. MacKay, S. T. Wilson, and M. C. Davey, "Comparison of constructions of irregular gallager codes," *IEEE Trans. Commun.*, vol. 47, pp. 1449–1454, Oct. 1999.

[23] B. Vasic, "High-Rate girth-eight low-density parity check codes on rectangular lattices," presented at the ICC'02, New York City, New York, Apr. 28–May 2, 2002.

[24] C. J. Colbourn and J. H. Dinitz, Eds., *The Handbook of Combinatorial Designs*. Boca Raton, FL: CRC, 1996.

[25] Y. Kou, S. Lin, and M. P. C. Fossorier, "Low-Density parity-check codes based on finite geometries: A rediscovery and new results," *IEEE Trans. Inform. Theory*, vol. 47, pp. 2711–2736, Nov. 2001.

[26] R. G. Gallager, *Low Density Parity Check Codes*. Cambridge, MA: MIT Press, 1963.

[27] E. Yeo, P. Pakzad, B. Nikolic, and V. Anantharam, "High throughput low-density parity-check decoder architectures," in *Proc. IEEE Global Telecommunications Conf., 2001, GLOBECOM'01*, vol. 5, 2001, pp. 3019–3024.

[28] Flarion. Vector-Low-Density Parity-Check (V-LDPC) Coding Solution Data Sheet. [Online]. Available: http://www.flarion.com/products/ldpc_data_sheet.pdf

[29] C. Howland and A. Blanksby, "A 220 mW 1 Gb/s 1024-bit rate-1/2 low density parity check code decoder," *Proc. 2001, IEEE Conf. Custom Integrated Circuits*, pp. 293–296, 2001.

[30] T. Richardson, A. Shokrollahi, and R. Urbanke, "Finite-length analysis of various low-density parity-check ensembles for the binary erasure channel," presented at the CTW'02, Sunibel, FL, May 18–25, 2002.

[31] D. J. C. MacKay and M. C. Davey, "Evaluation of gallager codes for short block length and high rate applications," presented at the IMA Workshop on Codes, Systems and Graphical Models, Minneapolis, MN, 1999.


**Bane Vasic** (S'92–M'93–SM'02) received the B.S., M.S., and Ph.D. degrees in electrical engineering from the University of Nish, Serbia, Yugoslavia, in 1989, 1991, and 1994, respectively.

From 1996 to 1997, he was a Visiting Scientist at the Rochester Institute of Technology and Kodak Research, both in Rochester, NY, where he was involved in research on optical storage channels. From 1998 to 2000, he was with Bell Laboratories, Lucent Technologies, where he was involved in research in read channel architectures and iterative decoding and low-density parity check codes. He was involved in development of codes and detectors for five generations of Lucent (now Agere) read channel chips. Currently, he is a Member of the Faculty of the Electrical and Computer Engineering Department, University of Arizona, Tucson. He is an author of more than 15 journal articles, more than 50 conference papers, and one book chapter "Read Channels for Magnetic Recording," in *The CRC Handbook of Computer Engineering* (Boca Raton, FL: CRC, 2000). His research interests include coding theory, information theory, communication theory, digital communications, and recording.

Dr. Vasic is a Member of the Editorial Board of the IEEE TRANSACTIONS ON MAGNETICS. He also serves as a Technical Program Chair of the IEEE Communication Theory Workshop 2003 and Co-Organizer of the Center for Discrete Mathematics and Theoretical Computer Science (DIMACS) Workshop on Optical/Magnetic Recording and Optical Transmission, 2003.

**Ivan B. Djordjevic** received the B.S., M.S., and Ph.D. degrees in electrical engineering from the Faculty of Electronic Engineering, University of Nish, Nish, Serbia, and Montenegro, Yugoslavia, in 1994, 1997, and 1999, respectively.

From 1994 to 1996, he was with the Faculty of Electronic Engineering, University of Nish, working on modeling and simulation of optical/digital communication systems. From 1996 to 2000, he was with the State Telecommunications Company, District Office for Networks, Nish, Serbia, where he was invol-

ved in digital transmission systems commissioning and acceptance, design, maintenance, installation, and connection . From 2000 to 2001, he was a Postdoctoral Fellow with the National Technical University of Athens, Greece, working on fiber nonlinearities, MAN, and WAN modeling and simulation. Then, in the second half of 2001, he was with TyCom US, Inc., where he was involved in receiver modeling for dense-wavelength-division-multiplexing (DWMD) systems. He is now with the University of Arizona, Tucson, working on low-density parity check codes and iterative decoding for long-haul transmission as well as on simulation and modeling of DWDM systems. He is an author of more than 60 publications in international journals and conference proceedings. His research interests include DWDM fiber-optic communication systems and networks, coding for optical communications, coherent optical communications, information theory, and statistical communication theory.

**Raymond K. Kostuk** (M'93) received the B.S. degree from the U.S. Coast Guard Academy, New London, CT, in 1972, the M.S. degree in optical engineering from the Institute of Optics, University of Rochester, Rochester, NY, in 1977, and the Ph.D. degree in electrical engineering from Stanford University, Stanford, CA, in 1986. His dissertation work focused on multiplexed holography and optical interconnects under the supervision of Joseph Goodman.

During his service with the U.S. Coast Guard (1972–1982), he worked at their Research and Development Center on vision and signaling problems. After completing the Ph.D. degree, he spent a year at the IBM Almaden Research Laboratory, working on optical data-storage-related problems. In 1987, he joined the faculty of the University of Arizona, Tucson, as an Assistant Professor with joint appointments in the Department of Electrical and Computer Engineering and the Optical Sciences Center. In 1997, he became a Full Professor in both departments. He has authored or coauthored more than 70 papers and presentations in the areas of holography and holographic recording materials, optical interconnects, planar optic systems, fiber-optic devices and systems, $\mu$-resonators and photonic bandgap devices, and optical data storage. He has also written four book chapters and holds a patent in these research areas.

Dr. Kostuk is a Fellow of the Optical Society of America (OSA).